

# 3 Dimensional Finite Element Simulation of Seam Welding Process

J. Saleem<sup>1</sup>, A. Majid<sup>1</sup>, K. Bertilsson<sup>1</sup>, T. Carlberg<sup>2</sup>

<sup>1</sup>Department of Information Technology and Media, Mid Sweden University,  
Holmgatan 10, 85170, Sundsvall, Sweden.

<sup>2</sup>Department of Material Engineering, Mid Sweden University,  
Holmgatan 10, 85170, Sundsvall, Sweden.  
jawad.saleem@miun.se

**Abstract**—The versatility, rich mathematical formulations and robustness of finite element methods make them attractive for simulations for a wide range of problems. Two dimensional models concerning the seam welding process do have some limitations. The longitudinal two dimensional models cannot be used to examine the effects of the electrode shape and thickness regarding heat generation during the seam welding process. The transversal two dimensional models are not helpful for examining the nugget growth during the seam welding process. The heat energy generated during the seam welding process mainly depends on the resistance between the electrodes, welding current, rotational speed and the geometry of the electrodes. The settings for appropriate parameters in relation to a seam welding machine, with regards to sheets of different thicknesses, depends on trial and error methods. These methods are expensive and time consuming. The three dimensional model developed in this paper is a step towards selecting the appropriate welding parameters so as to produce a good welding nugget.

**Index Terms**—Seam welding, finite element method, temperature dependent material properties, heat affected zone, weld nugget formation, inverter drive resistance welding equipment.

## I. INTRODUCTION

Resistance seam welding is a widely used process for joining metal sheets in the automobile industry. It is also used in the manufacturing of steel roofs in relation to water tightness. In all these applications leakage is not allowed and thus it is important for reliable welding procedures to be used. The important factors for maintaining consistency and a good seam weld nugget formation are, the welding force, welding current magnitude, welding speed, electrode shape and the mode of the current being supplied [1].

In seam welding, the electrodes used are in the form of rollers as shown in Fig. 1. The electrical current is passed through the roller shaped electrodes, which produces heat at the interface of the sheets which are to be joined. A seam welding process produces a series of nuggets at the interface of the steel sheets. The parts to be welded are placed between the circular electrodes, which run at a constant velocity in opposite directions and the squeeze force is

applied by these electrodes. The current produces a joule heating effect at the contact of the two sheets and the weld nugget is thus formed.

The weld joints formed by the seam welding machines are of three types as shown in Fig. 2. In the roll spot joint, as shown in Fig. 2(a), the weld schedule is fired at a constant repetition rate in order to form weld nuggets with distinct separation. If the linear velocity of the circular electrodes is maintained and the firing rate of the current supplied is increased, then the spots of the weld become closer together until they overlap forming the overlap joint as shown in Fig. 2(b). The overlapping of the nugget may vary from 10% to 50%. For gas tight joints the overlapping is from 40% to 50% and for a liquid tight joint it may vary from 10% to 40%. When the overlap is more than 50% then there is a continuous seam weld as shown in Fig. 2(c), and for which a continuous stream of energy is applied to the welding electrodes. The velocity of the circulating electrodes in the seam welder depends on the material being welded, the sheet thickness and also on the mode of current being applied. It is common practice in industry that the number of plates to be joined and the thickness of the sheets have a wide variation. To achieve the optimum weld control system parameters for different thicknesses of the steel sheets, repeated welds are made. The finite element model (FEM) is a useful tool for simulating the thermo-mechanical behaviour of the structures during welding [2]. Solving nonlinear equations in an electro-thermo-mechanical problem in a time stepping procedure such as for resistance welding requires high computational power.

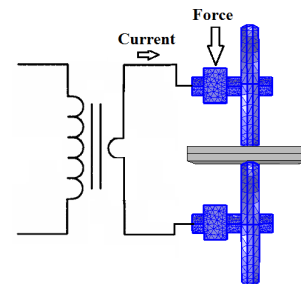


Fig. 1. Seam welding schematic.

Therefore the solution to such problems requires high computational capabilities. Progress in computer technology

associated with fast computing capabilities, huge memory and flexible communication have made it possible for them to be used in the following fields [3]:

- 1) Simulating physical phenomena by using numerical analysis;
- 2) Statistical analysis of experimental data;
- 3) Real time control manufacturing machines and experimental data.

The computational capability can, however, be reduced by making an efficient finite element model of the problem by reducing the dimensions of the model from three dimensions to two. FEM code for the solution of different problems can be developed by using a general set of subroutines provided by the software. The most popular softwares used to model the resistance welding process are ANSYS [4], JWRAIN [5] and ABAQUS [6]. About 90% of FEM programs are generic and use similar matrix solvers, quadrature rules and matrix assembly procedures. The seam welding problem is a three dimensional problem. A two dimensional model of a seam welding problem has been developed by [7], [8], in order to study the effect of current on the weld nugget formation. Their two dimensional model has been developed from the axisymmetric code developed for the spot welding process [9], [10]. The two dimensional representation of the seam welding process can be analyzed as a transverse cross section (2DT) or as a longitudinal cross section (2LT) as shown in Fig. 3.

To study the growth of the nugget in the longitudinal direction, a longitudinal model is suitable. The effect of the electrode size and shape on the overall weld can be observed by means of the transverse cross section model.

The quality of the seam weld joint is mainly dependent on the welding current, the pressure applied between the circular electrode wheels, the motor speed and the width of the welding wheels.

50 Hz thyristor controlled machines were previously used in industry, however, with the development of high powered semiconductor switches and DC-DC converter topologies, it is now possible to develop inverter drive resistance welding equipment, which can be operated at frequencies higher than the 50 Hz frequency. The advantage of using high frequencies is in relation to the reduction in the size of the welding transformer. The contact resistance at the faying surface is influenced by the electrode force. A higher pressure between the welding wheels demands a high current in order to achieve the same melting of the weld as compared to that for lower pressure settings. A slow welding speed in the seam welding process results in a wider weld because the welding material has more time to receive the heat generated by the welding current.

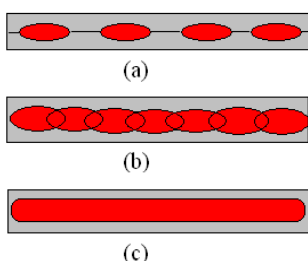


Fig. 2. Types of seam welding joints.

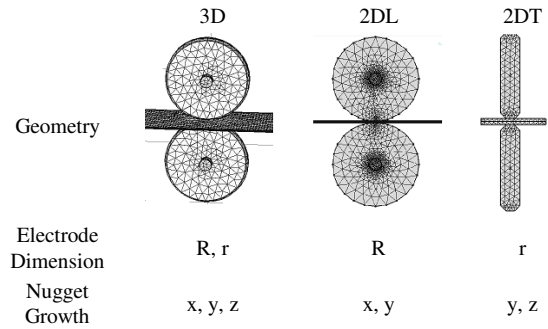


Fig. 3. Model types.

## II. SIMULATION MODEL

Two and three dimensional models for the seam welding process have been developed and analyzed by using COMSOL Multi-physics software. The geometrical specifications of the electrode wheels and the sheets are shown in Fig. 4. The COMSOL user interface reduces the clutter and redundant tasks, so that attention can be focused on the substance of the design studies, resulting in an increased productivity [11]. COMSOL Multi-physics provides a flexible platform which will even enable a new user to model the different physics involved in the design. The platform is also very adaptable and changing or adding new physics is very easy. It is also possible to readily introduce custom solver sequences and parameterized geometry into the design. Another advantage associated with the use of COMSOL Multi-physics is in relation to the built-in functions that contain a set of predefined routines such as analytical, step, ramp functions etc, which can be useful in applying the input to the system, for example, applying a current to the electrodes. The developed models involve three physics namely, electrical, heat transfer and structural mechanics. The structural mechanics module imposes a force, rotational speed and fixed boundary constraints on the modelled geometry. The electrical module controls the application of the required current to the electrodes. The electrode, work pieces and contact region are assumed to behave elasto-plastically. The heat transfer module governs the joule heat distribution as given in (1)

$$\rho C_p \partial T / \partial t = \nabla(k \nabla T) + Q_T, \quad (1)$$

where  $C_p$ ,  $\rho$ ,  $k$ ,  $Q_T$  are the specific heat, density, thermal conductivity, and heat source term per unit volume.

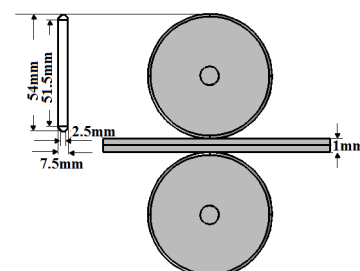


Fig. 4. Dimensions of the electrodes and sheets.

## III. FINITE ELEMENT

The geometry includes the circular copper electrodes and

steel sheets. In order to achieve a correct interpretation of the data in a finite element analysis, it should be properly meshed. The software has the capability to draw triangular, tetrahedral and quad meshes in the domains, and on the boundaries. It is also important, in time dependent models, to decide the time steps to resolve the wave equally well in time as the mesh does in space. The maximum allowed mesh element for the model can be given as in (2)

$$h_0 = \frac{C}{N \times F}, \quad (2)$$

where  $h_0$  is the size of the mesh element,  $C$  is the speed of light or sound,  $N = 5$  the number of mesh elements per wavelength. There is relationship between the time step and mesh size known as the  $CFL$  number. To achieve optimum solution, the value for the  $CFL$  is 0.2 [12]. Any smaller value of  $CFL$  will lead to shorter time steps resulting in long simulation times with no significant improvements in the solution. The time step  $T_s$  for the selected mesh can then be calculated as

$$T_s = \frac{CFL \times h_0}{C}. \quad (3)$$

In the simulation model, a normal tetrahedral mesh with 2740 and 16967 elements, respectively, are made for 2D longitudinal and 3D models.

#### IV. MATERIAL PROPERTIES

The seam welding process is complex involving physical, chemical and mechanical changes and it involves many phenomena such as, bulk joule heating, heat conduction, latent heat of fusion and phase changes. The materials involved in seam welding, namely the copper electrodes and the steel sheets, are subjected to a wide range of temperatures. Therefore, temperature dependent material properties are considered in the simulation. The electro-mechanical properties such as thermal conductivity, coefficient of thermal expansion, specific heat, and resistivity are taken as temperature dependents [13], [14].

#### V. COMPARISON OF 2-D AND 3-D SIMULATION

The seam welding simulation runs for 3 s when using electro-thermal-mechanical physics. The welding current is applied to the top electrode in the simulation as shown in Fig. 1, with the lower wheel grounded. The welding speed is 4 cm/s. The squeeze force applied during the simulation is 750 N for both two and three dimensional models.

The timed temperature distribution at the steel sheet interface can be a good indicator of the weld nugget formation. In the longitudinal two dimensional simulation, only the weld nugget growth from the cross section in the  $x, y$  domain can be observed as shown in the Fig. 5. This model has a limitation, because the effects of the electrode geometry in the  $y, z$  domain on the heat formation in the weld are not considered. However, a transverse two dimensional model can be used to overcome this limitation. Current intensity in amperes is used as the input for the

simulation. Longitudinal or transverse two dimensional simulation models also have limitations. These models cannot directly predict the exact amount of current intensity compared with the actual seam welding control system parameters.

The 3D model overcomes the limitations of 2D models because it does consider the 3D electrode geometry, and therefore can be used to directly predict the amount of welding current used for particular thicknesses of the sheets.

As shown in Fig. 6 the developed 3D model with temperature dependent material properties can be used to estimate the appropriate welding parameters such as the welding current, squeeze force and welding speed for the actual seam welding control system in order to obtain a good weld joint. The 3D model assists in analyzing the temperature distribution in the heat affected zone (HAZ) in the  $x, y$  and  $z$  dimensions. Moreover, the parametric surface selection can be used to define an ROI (region of interest) to observe changes in the temperature, stress, deformation and electric potential etc.

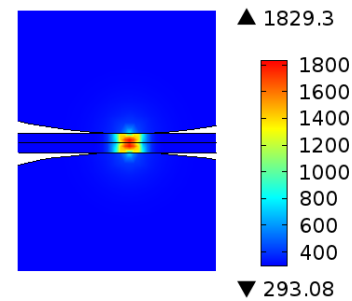


Fig. 5. Weld nugget for longitudinal 2D model.

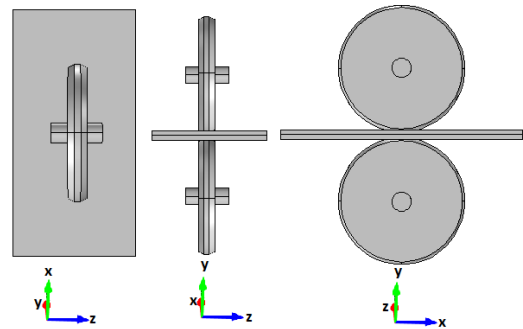


Fig. 6. 3D model orientations.

Figure 7(a) shows the parametric surface in the HAZ in the  $x, z$  axis, namely from the top side of the sheets. Figure 7(b) shows the HAZ from the transverse section showing the width of the HAZ under the electrode wheels in the  $y, z$  direction. The longitudinal section Fig. 7(c) shows the nugget formation during the seam welding process in the  $x, y$  direction. The developed model is also adaptable in relation to quick changes and it is possible to change the geometry of the electrode wheels. A parametric sweep can be used over the sheet thickness, in order to obtain the welding parameters for different thicknesses of the sheets. It is also very useful to run a parametric sweep over the welding parameters for a specific geometry and then plot and analyze all the results in order to obtain the best weld parameter settings for the welds in terms of strength.

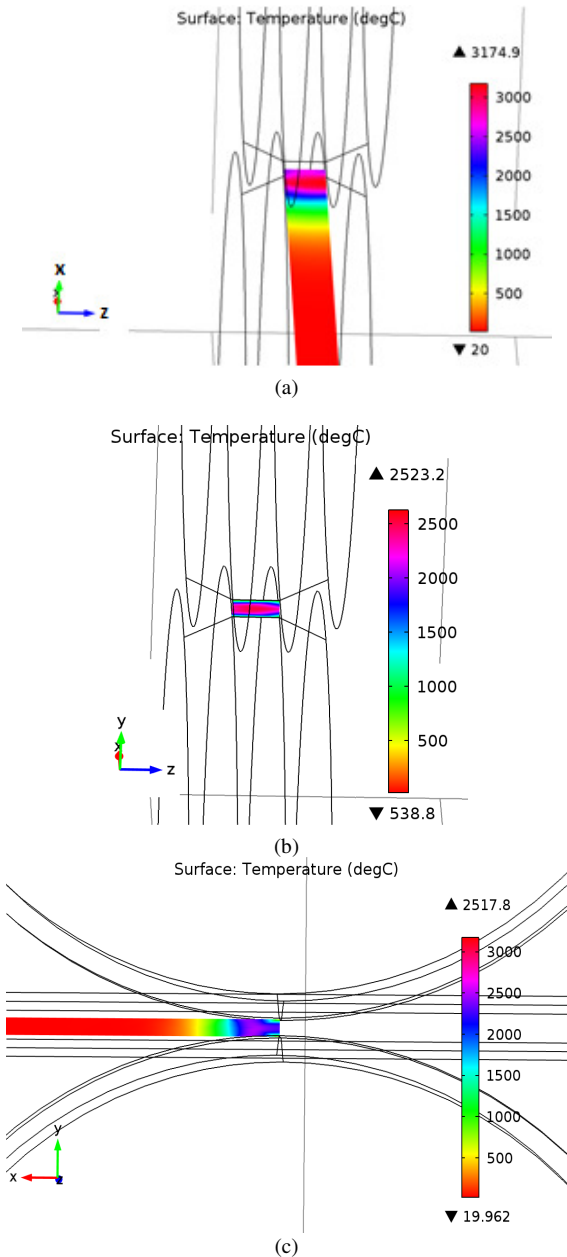


Fig. 7. Top view of nugget growth (a); transverse view of nugget growth (b); longitudinal view of nugget growth (c).

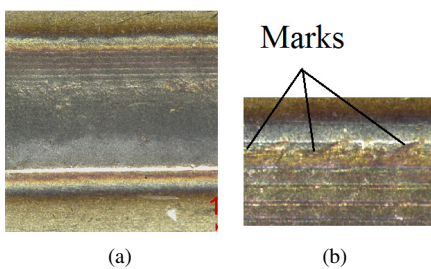


Fig. 8. Seam weld samples 50 Hz.

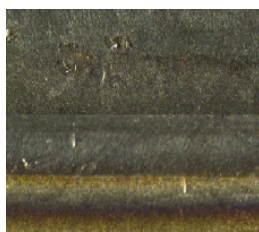
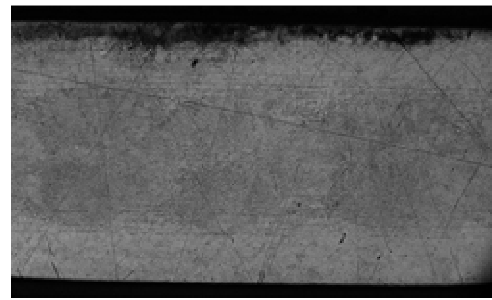
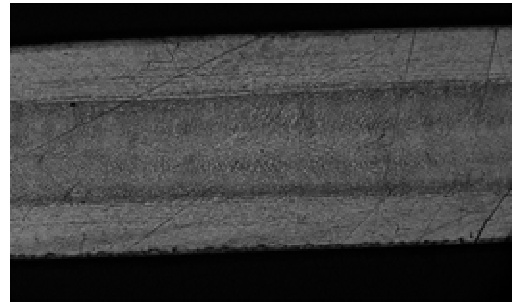


Fig. 9. Seam weld samples 400 Hz.



(a)



(b)

Fig. 10. Sample No:2 50 Hz 3.5kAmps (a); sample No:6 400 Hz 3.5kAmps (b).

## VI. EXPERIMENTS WITH 50HZ AND 400HZ WELDS

As mentioned previously in Section I, the inverter drive resistance seam welding equipment, which can be operated at frequencies higher than the 50 Hz frequency, is becoming a good choice for the welding industry, especially in relation to the stainless-steel roofing industry, because of its light weight. This offers an advantage to the user to have a light portable machine. The inverter based machine are also energy efficient than the conventional 50 Hz machines.

In the study conducted in this article, several weld samples were collected from both 50 Hz and 400 Hz.

The data from the experiments is shown in Table. I.

TABLE I. SEAM WELD SAMPLES

Sample number	Frequency	Current
1	50 Hz	2.7 kA
2	50 Hz	3.5 kA
3	50 Hz	2.9 kA
4	400 Hz	2.5 kA
5	400 Hz	2.8 kA
6	400 Hz	3.5 kA

Sample No. 2 and sample No. 6, which are taken at a current setting of 3.5 kAmp on both machines, are discussed in this section. A visual inspection of the joints is a feasible method for the stainless steel roofing industry, in order to judge the joint strength, as it is difficult to conduct run time destructive test for the welds.

A microscopic study of all the samples was performed. At first, the top surface of the welding joints was viewed using a microscope. A visual inspection shows that the melting of the material appears to be satisfactory in both the samples, based on the colour, as shown in Fig. and Fig.. However, all the 50 Hz samples displayed periodic marks on the edges of the weld zone which are not present in the 400 Hz samples as shown in Fig..

In the second phase, the samples were etched and polished. The weld zone for all the samples was observed. The samples showing the weld zone for both cases are shown in Fig. 10(a), and Fig. 10(b).

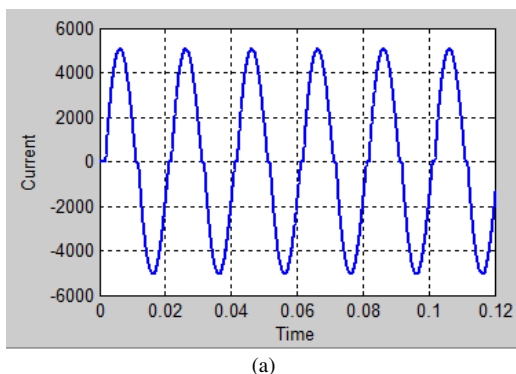
The dendritic in the melt zone can be either equiaxed or columnar depending on the solidification parameters, heat transfer, fluid flow, local thermal and solutal fields [15]. Equiaxed grains nucleate heterogeneously in all directions whereas, in columnar growth, the grains are preferentially oriented in one crystallographic direction parallel to the heat extraction from the melt. The columnar to equiaxed transition (CET) is defined as the change in the dendritic growth regime occurring during the solidification [16]. The CET depends on the nature of the composition of the metal, the heat formation during the welding and the cooling conditions. It is well known, from the mechanical point of view, that fine equiaxed grains are preferable to columnar grains [16].

Both sample No. 2 and sample No. 6 were observed using a higher magnification, and it was observed that in the 400 Hz machine sample, as shown in Fig. 11, a columnar zone is formed, at the point where columnar grains meet in the centre.

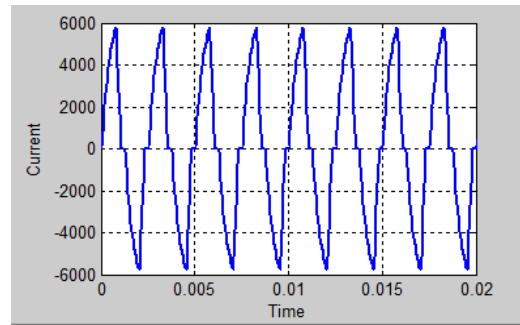


Fig. 11. Magnified image of the sample No. 6.

This does not correspond to a very good joint in terms of strength because a weak zone is formed where the grains meet. Both the 50 Hz and 400 Hz machines were supplied with a continuous current mode signal of 3.5 kAmp as shown in the Fig. 12(a) and Fig. 12(b) respectively. The same signals were applied as input to the developed 3D FEM model in order to observe the heat formation during the welding process. The thermal profile of the point, considered at the steel sheet interface for both cases, is shown in Fig. 13. It can be observed from the thermal profile of the 50 Hz simulation that, a periodicity exists in the heat formation with the same frequency as seen in the micrographs of the actual weld samples 1, 2 and 3.



(a)



(b)

Fig. 12. 50 Hz continuous current mode (a); 400 Hz continuous current mode (b).

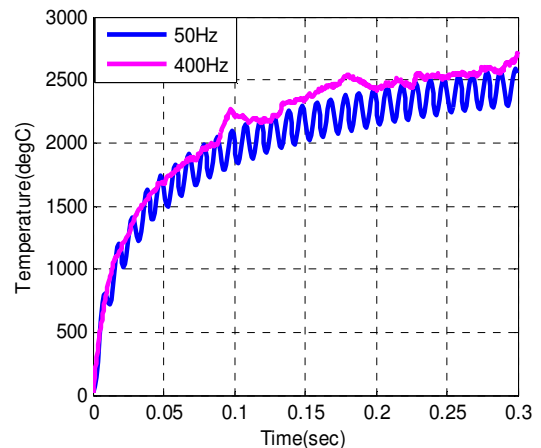


Fig. 13. Heat profile for continuous current mode 50 Hz and 400 Hz.

This cooling effect plays an important role in the dendritic growth. The thermal profile of the 400 Hz FEM simulation shows a continuous rise in the temperature resulting in overheating, induced by an increase in the total heat input.

In order to achieve heat formation in the 400 Hz machine which is similar to that for the 50 Hz machine, one possible solution is to apply the input current signal in burst mode. This will introduce periodicity into the current signal of the 400 Hz machine. For this purpose, a circuit simulation of both 50 Hz thyristor based and 400 Hz inverter based systems has been developed in MATLAB/Simulink. The signals in Fig. 12(a), Fig. 12(b) show the continuous mode current delivered to the electrode wheels. In the case of the inverter based 400 Hz machine, the IGBT in the full bridge circuit are ON for 30% of the time period.

For the burst scheme, the IGBT duty cycle is increased to 45% so as to compensate for the OFF cycles, in order to have the same RMS current magnitude i.e. 3.5 kAmps. Two burst schemes are proposed:

- 1) Six ON two OFF cycles;
- 2) Three On one OFF cycles.

These two schemes are shown in Fig. 14(a) and Fig. 14(b) respectively. Both the signals are applied as input to the seam welding FEM model. The heat profile at the two steel sheet interfaces is observed. Figure 15 shows the heat profile of the burst mode with three ON and one OFF together with 50 Hz continuous and 400 Hz continuous mode input signals.

The heat profile of the burst signal in this case is similar to that for the 50 Hz machine. The heat generation also shows the periodicity with the same frequency. The heat

profile of the six ON and two OF scheme is almost similar, but, the frequency is half that of the 50 Hz.

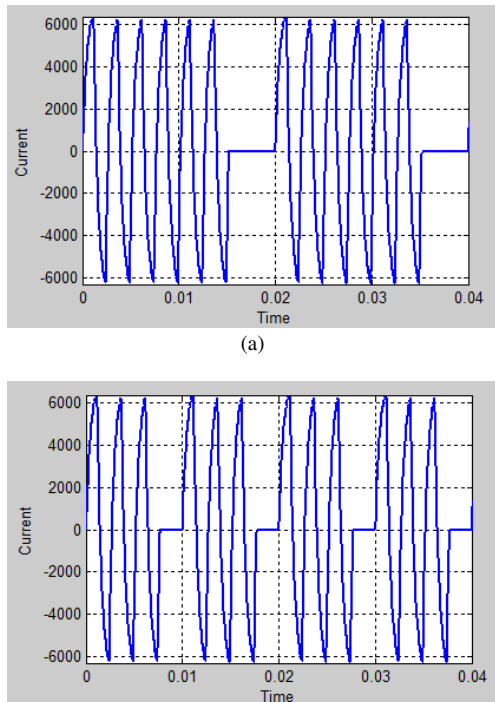


Fig. 14. 400 Hz 45% duty cycle burst signal (a); 400 Hz 45% duty cycle burst signal (b).

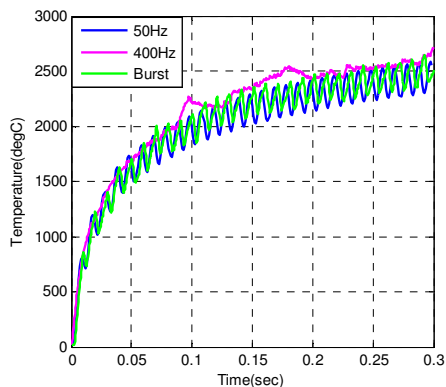


Fig. 15. Heat profile for continuous current mode 50 Hz and 400 Hz and with ON one OFF.

## VII. CONCLUSIONS

Advancements in numerical tools and the increased computational capability of computers have made it possible for them to be used in research in order to model complex problems such as welding. The two dimensional seam welding model requires less complex geometry and has less computational requirements. On the other hand, these models have limitations in relation to studying the weld nugget formation during the seam welding process. The longitudinal two dimensional can be useful only in determining the heat formation in the longitudinal direction. The transverse two dimensional model can be used to view the effects of the shape of the welding electrode wheel on the weld nugget growth.

The inverter based seam welding machines are more energy efficient than the conventional 50 Hz machines but, the experimental results show that, in the samples taken from the 400 Hz machine, a columnar zone is formed, where

columnar grains meet in the centre and therefore a weak zone is formed. This can be avoided by controlling the overheating formation during the seam welding process, produced by the input current. A current with a discontinuous mode could be the preferable choice in order to produce a stabilized contact state that may avoid columnar growth.

A three dimensional model with accurate material properties for the seam welding could prove to be a good tool for understanding the difference between applying different frequency/mode input signals and in checking their effect on the seam weld nugget growth. It is possible to observe changes in the HAZ in the developed simulation for very short time intervals of perhaps a few milliseconds which may not prove to be possible to observe in the case of real welds.

## REFERENCES

- [1] M. J. Karagoulis, *Welding, Brazing, and Soldering (ASM International, Handbook, vol. 6)*. General Motors Corporation, 1993, pp. 238–246.
- [2] L. E. Lindgren, “Finite element modeling and simulation of welding part 1: Increased complexity”, *Journal of Thermal Stresses*, vol. 24, no. 2, 2001. [Online]. Available: <http://dx.doi.org/10.1080/01495730150500442>
- [3] Y. Ueda, H. Murakawa, “Application of Computers and Numerical Analysis Techniques in Welding Research”, *Technical review Transaction of JWRI*, vol. 13, no. 2, 1984.
- [4] A. G. Thakur, A. R. Rasane, V. M. Nandedkar, “Finite element analysis of resistance spot welding nugget formation” *Int. Journal of Applied Engineering and Research, Dindigul*, vol. 1, no. 3, 2010.
- [5] M. A. Ninsu, H. Murakawa, “Numerical and Experimental Study on Nugget Formation in Resistance Spot Welding for High Strength Steel Sheets in Automobile Bodies”, *Trans. of Joining and Welding Research Institute (JWRI)*, vol. 38, no. 2, 2009.
- [6] J. A. Khan, L. Xu, Y. J. Chao “Prediction of nugget development during resistance spot welding using coupled thermal-electrical-mechanical model”, *Science and technology of welding and joining*, vol. 4, no. 41, 1999.
- [7] H. Murakawa, H. Minami “Development of Finite Element Method for Seam Welding and Its Application to Optimization of Welding Condition” *Proc. of the twelfth Int. Offshore and Polar Engineering Conference*, Kitakyushu, Japan, May 2002.
- [8] H. Murakawa, H. Minami, T. Kato “Finite Element Simulation of Seam Welding Process”, *Trans. JWRI*, vol. 30, no. 1, pp. 111–117, 2001.
- [9] H. Murakawa, H. Kimura, Y. Ueda, “Weldability Analysis of spot welding on Aluminium using FEM” *Trans. JWRI*, vol. 28, no. 1, pp. 41–46, 1999.
- [10] H. Murakawa, J. Zang, H. Minami, “FEM simulation of spot welding process (Report III) Controlling of welding current using electrode displacement for formation of large enough nugget without expulsion”, *Trans. JWRI*, vol. 28, no. 1, pp. 101–111, 1995.
- [11] *COMSOL Multiphysics*. [Online]. Available: [http://chemelab.ucsd.edu/CAPE/comsol/Comsol\\_API\\_Ref.pdf](http://chemelab.ucsd.edu/CAPE/comsol/Comsol_API_Ref.pdf)
- [12] *COMSOL Convergence tips*. [Online]. Available: <https://community.cmc.ca/docs/DOC-1453>
- [13] G. Zhong, “Finite element analysis of resistance spot welding process”, *Chinese Control and Decision Conference, CCDC*, 2009.
- [14] Z. Houa, S. Kimb, Y. Wanga, C. Lic, C. Chena, “Finite element analysis for the mechanical features of resistance spot welding process”, *Journal of Materials Processing Technology*, vol. 185, pp. 160–165, 2007. [Online]. Available: <http://dx.doi.org/10.1016/j.jmatprotec.2006.03.143>
- [15] Z. Gabalcová, J. Lapin, “Experimental study of columnar to equiaxed transition during directional solidification of Intermetallic Ti-46Al-8Nb Alloy”, *METAL*, 2009.
- [16] D. Montiel, L. Liu, L. Xiao, Y. Zhou, N. Provatas, “Microstructure analysis of AZ31 magnesium alloy welds using phase-field models”, *Acta Materialia*, vol. 60, no. 16, pp. 5925–5932, Sept. 2012. [Online]. Available: <http://dx.doi.org/10.1016/j.actamat.2012.07.035>